BMC Microbiology

RESEARCH Open Access

Metagenomics reveals seasonal changes of intestinal microbes in *Eospalax rothschildi*

Yao Zou[1,2,3], Quan Zou[1], Yansu Wang[1*] and Chongxuan Han[2*]

Abstract

Background Seasonal behavioral divergence in zokors, driven primarily by their reproductive cycle, results in distinct ecological strategies between breeding and non-breeding periods. To elucidate how intestinal microbes adapt to these behavioral shifts, we used metagenomics to characterize the seasonal variations in the intestinal microbes of *Eospalax rothschildi*, a subterranean zokor endemic to China.

Results Metagenomics revealed that summer samples showed an increased proportion of carbohydrate-degrading bacteria. Moreover, a significant difference in taxonomic composition was observed between the samples collected in the two seasons. Functional analysis based on the KEGG and CAZy databases revealed stronger carbohydrate degradation capacities in summer samples, notably through enhanced galactose metabolism capabilities. The enhanced galactose metabolism capabilities observed in summer were predominantly driven by increased abundance of α-galactosidase and β-galactosidase genes from enriched microbial populations, particularly *Bacteroides*, *unclassified_f_Lachnospiraceae*, *Roseburia*, and *Faecalibacterium*. Furthermore, iCAMP analysis revealed that deterministic and stochastic processes jointly governed intestinal microbial assembly in *E. rothschildi* during summer, as elevated nutritional demands potentially intensified host selection in the breeding season. Conversely, stochastic dominance in autumn may align with relaxed host selection.

Conclusions Collectively, these results demonstrated that season played a crucial role in modulating the composition, function, and assembly process of the intestinal microbes of *E. rothschildi*.

Keywords Intestinal microbes, Metagenomics, Carbohydrate metabolism, Galactose metabolism, Seasonal changes

Background

Mammalian intestinal microbes and their hosts have developed a mutually beneficial symbiotic relationship over a long period of co-evolution. The genome of mammalian intestinal microbes encodes approximately 150 times more genes compared to that of their hosts. These microbes exert a profound influence on host biology through their interactions with the host [1]. Both the hosts and the microbiome can benefit from their interactions [2]. The host provides a stable and nutrient-rich place that promotes the establishment of microbial communities. It selectively facilitates the colonization of certain microbes by eliminating pathogenic bacteria while

*Correspondence:
Yansu Wang
wangyansu@uestc.edu.cn
Chongxuan Han
13564959975@163.com
[1]Institute of Fundamental and Frontier Sciences, University of Electronic Science and Technology of China, Chengdu 610054, China
[2]Key Laboratory of National Forestry and Grassland Administration on Management of Western Forest Bio-Disaster, Northwest Agriculture and Forestry University, Yangling 712100, China
[3]Quzhou Affiliated Hospital of Wenzhou Medical University, Quzhou Peoples Hospital, Quzhou, Zhejiang, China

permitting the survival of beneficial ones [3]. Intestinal microbes play a pivotal role in the intestinal nutritional metabolism. They fulfill their function by supplementing the digestive capacity of the host [4], which is necessary for the host to efficiently digest food, maintain homeostasis, and adapt to various environments [5–8]. Moreover, intestinal microbes and related metabolites possess a multitude of physiological functions. Specifically, they are involved in modulating host metabolism and immune response, maintaining intestinal barrier, repairing the intestinal epithelium, and exerting an influence on the expression of host genes [9–11]. Therefore, a comprehensive understanding of host-microbial interactions is of great significance for exploring the ecology and evolution of wildlife [12].

Increasing evidence indicates that, apart from host factors such as host genotype, phylogeny, and ecology, the composition and diversity of mammalian intestinal microbes are considerably influenced by environmental factors [10, 13–17]. These environmental variables comprise dietary [18, 19], seasons [20], lifestyle, social networks, environmental microbes [21], and geography [22]. Previous studies have demonstrated that diet plays an important role in shaping the gut microbiota [19, 23, 24]. It is common for wild animals to change their dietary patterns across different seasons and habitats, an alteration that potentially impacts their intestinal microbes. For example, seasonal changes in the rumen microbes of yaks facilitate their hosts' survival during shortages and exposure to cold stress in the spring and winter [25]. The composition and diversity of the intestinal microbes in wild Tibetan macaque also exhibited seasonal changes to adapt to seasonal fluctuations in food availability [26]. Similarly, the gut microbial composition of plateau pika demonstrated seasonal variations, which were correlated with the shifts in food nutrition across different seasons [27]. However, it remains uncertain whether seasonal changes in gut microbial composition of the host are concomitant with functional transformations. Additionally, the relevant studies are relatively limited.

Eospalax rothschildi, a typical subterranean zokor endemic to China, spends most of its life in underground tunnel systems. This species inhabits the Qinba mountains, a region characterized by warm-humid climate, fertile soils, and abundant plant resources [28]. Studies have demonstrated that the behavioral patterns of zokors exhibit seasonal differences, primarily driven by their reproductive cycle and manifesting as distinct ecological strategies between breeding and non-breeding seasons [29–31]. To resolve how intestinal microbes adapt to these seasonal transitions, we employed metagenomics to elucidate compositional and functional shifts in the intestinal microbes of *E. rothschildi* across seasonal transitions. Investigating the seasonal changes in the intestinal microbes of *E. rothschildi* is beneficial for understanding its nutritional demands in different seasons, thereby facilitating a more profound understanding of its habitat and dietary strategies. This study is expected to offer novel insights for the future development of ecological control measures against rodent damage.

Methods

Sample collection

Adult wild zokors (*E. rothschildi*, ER) were captured from Zhenba county (ZB, 32.5008°N, 108.0207°E), Shaanxi Province, China. The sampling region is situated within the Qinba mountains, where the mean annual temperature registers at 13.8 °C and the annual precipitation amounts to 1300 mm. The sample information was shown in Table S1. After being sedated with xylazine hydrochloride (5 mg/kg), the zokors were humanely euthanized by an intravenous overdose of pentobarbital sodium (390 mg/mL). The cecal contents were collected within 5 min and promptly transferred into cryogenic vials, frozen with liquid nitrogen, and subsequently stored in a laboratory freezer at −80℃. A total of seven cecal samples were collected, comprising four samples from the summer season (ER_S, $n = 4$) and three samples from the autumn season (ER_A, $n = 3$). Furthermore, the dominant plants in the sampling area of *E. rothschildi* were identified based on morphological characteristics. In both summer and autumn, plants were dominated by *Artemisia argyi*, *Plantago depressa*, and *Fragaria nilgerrensis*.

DNA extraction, PE library construction, and sequencing

Total genomic DNA was isolated from the cecal contents of zokors following the protocol provided by the Stool Genome DNA Extraction Kit (Tiangen Inc.). The DNA concentration was quantified using the Nanodrop 2000 Spectrophotometer (Thermo Fisher Scientific, Wilmington, NC, USA). Subsequently, DNA fragments were separated by 1% agarose gel electrophoresis and stained with ethidium bromide, and then visualized under UV light. After purifying with a gel extraction kit (Takara Bio Inc.), the DNA was submitted to Majorbio Bio-Pharm Technology Co. Ltd. (Shanghai, China) for sequencing.

To initiate the library construction process, the DNA was fragmented to approximately 400 bp in length using Covaris M220 instrument (Gene Company Limited, China). Thereafter, paired-end library was assembled with the NEXTFLEX Rapid DNA-Seq Kit (Bioo Scientific, Austin, TX, USA). Adapters containing the full complement of sequencing primer hybridization sites were ligated to both ends of fragments. Paired-end sequencing was carried out on the Illumina NovaSeq platform (Illumina Inc., San Diego, CA, USA) at Majorbio Bio-Pharm Technology Co., Ltd. (Shanghai, China) using NovaSeq

Reagent Kits following the manufacturer's instructions (www.illumina.com).

Sequence quality control and genome assembly

The paired-end Illumina reads were performed using Kneaddata v0.7.4. This involved performing quality filtering with Trimmomatic v0.39 [32], and removing host-derived sequences by aligning to the reference genome of closely related species (*E. fontanierii*, GCA_035773235.1) using Bowtie2 v2.3.5.1 [28, 33].

Metagenomic data assembly was carried out using Megahit v1.2.9 [34]. Genome assembly evaluation using QUAST v5.0.2 generated 6.85 million contigs spanning 7.29 Gbp total length, with an N50 value of 1,059 bp. Considering the balance of data quality and computational efficiency, we choose a length of 500 bp as the filtering threshold. Contigs with a length of no less than 500 bp were chosen as the final assembled contigs and subsequently utilized for further gene prediction and functional annotation. Summary statistics on sequence quality control and assembly of each sample were presented in Table S2.

Gene prediction, taxonomy, and functional annotation

The prodigal software v2.6.3 [35] was used to predict open reading frames (ORFs) within each assembled contig. Subsequently, CD-HIT v4.8.1 was utilized to construct non-redundant gene sets with 95% identity based on the predicted ORFs [36, 37]. Clean reads were then mapped to the non-redundant gene sets to compute gene abundance with Salmon v1.2.1 [38]. Furthermore, the EMBOSS software v6.6.0.0 was engaged to translate the non-redundant gene sequences into non-redundant protein sequences for the purpose of annotation.

Representative sequences of non-redundant gene sets were mapped to the NR database with an e-value cutoff of $1e^{-5}$ by employing Diamond v0.8.22 for taxonomic annotation purposes [39]. Subsequently, all valid sequences for all samples were annotated via Kraken2 v2.0.7-beta [40]. Moreover, the relative abundance of each sample at the genus level was estimated using Bracken v2.0 [41].

Non-redundant gene sets were aligned to the KEGG (http://www.genome.jp/kegg/) database and the CAZy database (http://www.cazy.org/) with an e-value cutoff of $1e^{-5}$ using Diamond v0.8.22 for functional annotations [42]. EggNOG-mapper v2.0.1 was used to compare the non-redundant protein sequences with the EggNOG database to obtain the functional annotations [43].

The abundance (TPM) of non - redundant genes annotated to the same gene family was aggregated to generate a feature table in the database. Additionally, the alpha diversity and the beta diversity were estimated at the genus level. Moreover, the microbes encoding glycoside hydrolases (GHs) at the genus level were analyzed and counted.

Metagenomic binning

Assembled contigs with a length of no less than 1000 bp were subjected to binning using Metabat v2.12.1 [44], Concoct v0.5.0 (https://github.com/BinPro/CONCOCT), and Maxbin v2.2.5 (https://sourceforge.net/projects/maxbin/). Subsequently, the obtained bins were refined via RefineM v0.0.24 [45]. The completeness and contamination levels of each bin were then evaluated by CheckM v1.0.12 [46]. All the bins were aggregated and subsequently dereplicated using dRep v2.2.9 [47]. These bins were classified using GTDB-tk v2.3.0 [48], which leverages 120 bacterial and 53 archaeal conserved marker genes from GTDB database. A phylogenetic tree was subsequently reconstructed based on these conserved genes. Moreover, the relative abundance of the bins was estimated by CoverM v0.6.1 (https://github.com/Ecogenomics/CheckM).

Microbial community assembly analysis

To infer the assembly processes of the microbial community across different seasons in *E. rothschildi*, we employed a phylogenetic bin-based null model via the "iCAMP" package in R to assess the relative contributions of ecological processes [49]. The Raup-Crick index (RCI) and β-nearest taxon index (βNTI) were computed to quantify the relative contributions of diverse processes [50]. A |βNTI| value of no less than 2 implies that deterministic processes dominate in the community assembly. Conversely, a |βNTI| value of no more than 2 suggests that stochastic processes dominate in shaping microbial communities. Subsequently, we integrated βNTI and RCI to estimate the relative strengths of various processes, namely homogeneous selection (βNTI < – 2), heterogeneous selection (βNTI > 2), drift (|βNTI| < 2 and |RCI| < 0.95), homogeneous dispersal (|βNTI| < 2 and RCI <–0.95) and dispersal limitation (|βNTI| < 2 and RCI >0.95), in driving the microbial community.

Statistical analysis and visualization

Differences in taxonomic composition and functional pathway abundances between groups were analyzed using two-tailed Wilcoxon rank-sum tests with significance defined at $p < 0.05$. The statistical results for each database were visualized as bar plots using ggplot2 in R v4.3.1. Based on genus-level abundance profiles, alpha diversity (Shannon index and Simpson index) and beta diversity (PCoA) were calculated using the vegan package (v2.6-4) in R. Inter-group comparisons of alpha diversity indexes were performed via two-tailed Wilcoxon rank sum tests with a significance threshold of $p < 0.05$. Microbial community structure differentiation between groups

was assessed through PERMANOVA (999 permutations) based on Bray-Curtis dissimilarity matrices, with statistical significance defined at $\alpha = 0.05$.

Results

The composition and diversity of intestinal microbes of *E. rothschildi* between the two seasons based on the NR database

After quality control and host DNA removal, 70.77% of raw reads per sample (mean sequencing depth = 3.1×) were retained across seven zokor samples for downstream taxonomic and functional annotation.

The annotations at the kingdom and family levels were shown in Fig. S1 and Fig. S2, respectively. The intestinal microbes of all zokor samples were dominated by bacteria with a mean relative abundance of 99.11%, followed by fungi (0.45%), and viruses (0.33%).

At phylum level, Bacillota and Bacteroidota were the main phyla in the intestinal microbes of *E. rothschildi* with a mean relative abundance of 66.91% and 16.35% respectively, followed by Pseudomonadota (10.39%) (Fig. 1a). At genus level, *Escherichia* (7.93%), *Dysosmobacter* (9.50%), *unclassified_o_Eubacteriales* (8.69%), *Lactobacillus* (7.64%), *Pseudoflavonifractor* (5.49%), *Streptococcus* (5.69%), *unclassified_f_Oscillibacter* (4.90%) were dominant microbes in zokor samples (Fig. 1b).

At phylum level (Fig. 1c), the proportions of Bacillota in summer and autumn were 76.77% and 53.77%, respectively, while the proportions of Bacteroidota were 5.84% and 30.37%, respectively. The proportion of Bacillota in *E. rothschildi* was significantly enriched in summer ($p < 0.05$). At genus level (Fig. 1d), the *Pseudoflavonifractor* was significantly enriched in summer ($p < 0.05$), and its relative abundance in summer and autumn were 7.67% and 2.59%, respectively.

Shannon and Simpson indexes were estimated as alpha diversity based on microbial relative abundance at genus level. By comparing the difference in alpha diversity between the two seasons, we have found that both the

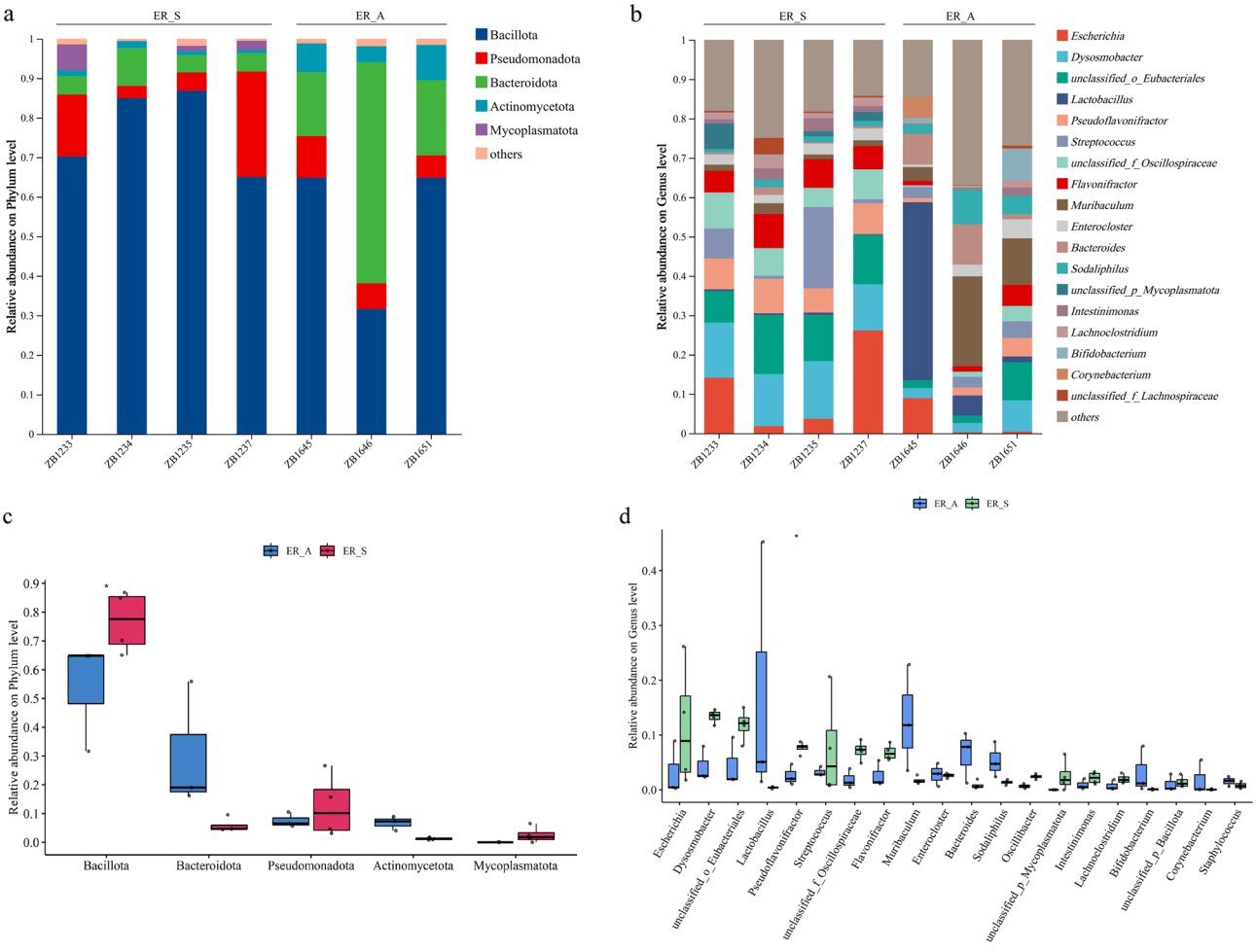

Fig. 1 Mean relative abundances of microbes (**a**) at phylum level and (**b**) at genus level across all zokor samples. Differences of intestinal microbial composition of *E. rothschildi* between the two seasons (**c**) at phylum level and (**d**) at genus level

Shannon and Simpson index did not differ significantly between the two seasons (Fig. S3a, $p > 0.05$).

Principal coordinate analysis (PCoA) was performed based on Bray-Curtis distance to visualize the difference in taxonomic composition of zokor intestinal microbes across different seasons. The result showed that the *E. rothschildi* from summer and autumn had distinct composition of intestinal microbes (Fig. S3b). PERMANOVA tests based on Bray-Curtis distance showed that season significantly explained 48.70% ($F = 4.74$, $R^2 = 0.4870$, $p < 0.05$) of the beta diversity among samples.

Intestinal microbial function of *E. rothschildi* between the two seasons based on the KEGG database

In KEGG pathway, the metabolic pathway at the first level was mainly divided into 6 categories (Fig. S4), including metabolism, genetic information processing, cellular processes, human diseases, environmental information processing, and organismal systems. More than 60% of the annotated genes were associated with metabolism (Fig. S4). We mainly focused on the metabolism.

The relative abundance of intestinal microbial function between the two seasons at the second level of KEGG pathway under metabolism was shown in Fig. 2a. Among them, the metabolic pathways mainly contained 13 functions, while carbohydrate metabolism was the most abundant with the mean relative abundance of 11.03%, followed by amino acid metabolism (9.52%), and metabolism of cofactors and vitamins (9.00%). By comparison of differences in metabolic pathways between the two seasons, carbohydrate metabolism was significantly enriched in summer than that of autumn (Fig. S5, $p < 0.05$).

The relative abundance of intestinal microbial function between the two seasons at the third level of KEGG pathway under carbohydrate metabolism was shown in Fig. 2b. The dominant pathway of all zokor samples was citrate cycle _TCA cycle, followed by pyruvate metabolism, glycolysis/gluconeogenesis, starch and sucrose metabolism, and galactose metabolism. The pathway of starch and sucrose metabolism (ko00500), and galactose metabolism (ko00052) in *E. rothschildi* were both significantly enriched in summer (Fig. 2b, $p < 0.05$). The enrichment of genes related to carbohydrate metabolism in summer was likely reflected through the enrichment of starch and sucrose metabolism, and galactose metabolism.

The metabolic pathway of galactose metabolism (ko00052) involves a variety of carbohydrate metabolic processes, and various enzymatic reactions (Fig. S6). Based on the annotations in KEGG Enzyme, the top eight abundant enzymes involved in galactose metabolism were shown in Fig. 2c. Among them, α-galactosidase (EC 3.2.1.22) was the most abundant enzyme in galactose metabolism with the mean relative abundance of 0.16%. By comparing the differences between the two seasons, the results showed that α-galactosidase (EC 3.2.1.22), β-galactosidase (EC 3.2.1.23), galactonate dehydratase (EC 4.2.1.6), and tagatose 1, 6-diphosphate aldolase (EC 4.1.2.40) were significantly enriched in summer (Fig. 2c, $p < 0.05$). These results suggested that the enrichment of galactose metabolism in summer was mainly reflected by the enrichment of genes coding for α-galactosidase and β-galactosidase.

Seasonal differences in the abundance of galactosidase-encoding genes from various GH families based on the CAZy database

As shown in Fig. S7, the genes were divided into 6 classes based on CAZy database. The 6 classes include glycoside hydrolases (GH), glycosyl transferases (GT), carbohydrate binding modules (CBM), polysaccharide lyases (PL), carbohydrate esterases (CE), and auxiliary activities (AA). Among them, GH was the most abundant function (Fig. S7), and galactosidase belonged mostly to GH.

To verify intestinal microbial functions related to galactose metabolism in *E. rothschildi*, we targeted genes encoding α-galactosidase or β-galactosidase from

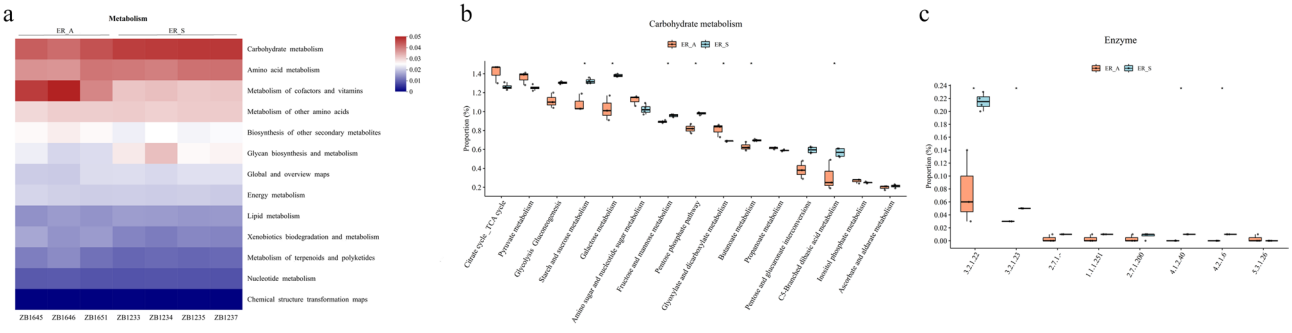

Fig. 2 The functional comparison of intestinal microbes of *E. rothschildi* between the two seasons based on KEGG pathway database. **a** Heatmap showing the intestinal microbial function of *E. rothschildi* across all samples at the second level under KEGG metabolism pathway. **b** Differences of intestinal microbial function of *E. rothschildi* between the two seasons at the third level under KEGG carbohydrate metabolism pathway. **c** Differences of enzyme genes of *E. rothschildi* in galactose metabolism pathway (ko00052) between the two seasons

various GH families to assess changes in relative abundance across seasons. Results indicated that the relative abundance of α-galactosidase genes from GH31, GH4, GH57, GH27, GH36, and GH97 families was higher in summer samples, while only GH31 showed a significant difference in abundance between seasons (Fig. 3a, Wilcoxon rank sum test, $p < 0.05$). Similarly, the relative abundance of β-galactosidase genes from GH1, GH2, and GH42 families was increased in summer, although only GH2 exhibited a significant difference in abundance (Fig. 3b, Wilcoxon rank sum test, $p < 0.05$). Therefore, α-galactosidase genes of GH31 and β-galactosidase genes of GH2 were identified as differentially abundant galactosidase genes (Fig. 3). These results indicated that the relative abundance of both α-galactosidase and β-galactosidase genes from some GH families was higher in summer than in autumn.

Inference of dominant microbes encoding differentially abundant galactosidase genes from various GH families

Through integrated annotation, we screened for genes that were assigned to a genus-level taxonomy in the NR database and were also identified as differentially abundant galactosidase genes from various GH families in the CAZy database. These genus-level microbes were inferred to encode differentially abundant galactosidase genes from various GH families. Integration with gene abundance profiles enabled the identification of dominant microbes encoding these differentially abundant galactosidase genes in each sample. Dominant microbes inferred to encode differentially abundant α-galactosidase genes from the GH31 family included *Bacteroides*, *unclassified_f_Lachnospiraceae*, *unclassified_c_Clostridia*, *Roseburia*, *unclassified_f_Bacteroidaceae*, *unclassified_o_Eubacteriales*, *Lactobacillus*, *unclassified_f_Muribaculaceae*, *Blautia*, and *unclassified_o_Bacteroidales* (Fig. 4a). Among them, the proportion of *Bacteroides*, *unclassified_f_Lachnospiraceae*, *unclassified_c_Clostridia*, *Roseburia*, and *unclassified_f_Muribaculaceae* was higher in summer, while the proportion of *Lactobacillus* was higher in autumn (Fig. 4a).

Moreover, dominant microbes inferred to encode differentially abundant β-galactosidase genes from the GH2 family included *unclassified_f_Lachnospiraceae*, *Faecalibacterium*, *unclassified_o_Eubacteriales*, *unclassified_c_Clostridia*, *unclassified_f_Oscillospiraceae*, *Mediterraneibacter*, *unclassified_f_Bacteroidaceae*, *Bacteroides*, *Hungatella*, and *Roseburia* (Fig. 4b). Among them, the proportion of *unclassified_f_Lachnospiraceae*, *Faecalibacterium*, *unclassified_o_Eubacteriales*, and *unclassified_f_Oscillospiraceae* was higher in summer, while the proportion of *Mediterraneibacter*, and *Hungatella* was higher in autumn (Fig. 4b).

Metagenomic binning

Using CheckM v1.0.12 for quality assessment, we obtained 97 medium-quality genomic bins (≥ 50% completeness, ≤ 10% contamination) with mean completeness of 77.6% ± 13.1% and contamination of 2.8% ± 2.4%. Using GTDB-tk v2.3.0 with the GTDB v214.1 reference database, most bins were taxonomically assigned up to the family-level resolution (Table S3). Only one bin (MAG5, 76.84% completeness, 1.4% contamination) was annotated to species-level (*Treponema_D sp017935745*). The phylogenetic relationships and family-level taxonomy of 97 bins from zokor gut were shown in Fig. S8. The relative abundance of bin-based taxa of all zokors at

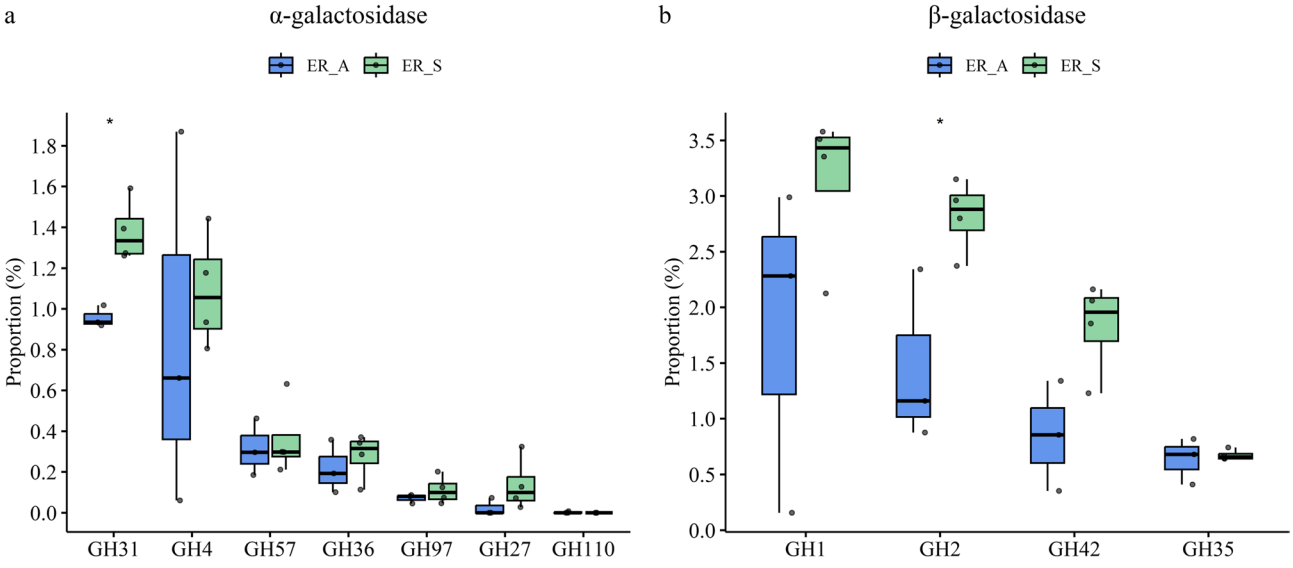

Fig. 3 The relative abundance of (**a**) α-galactosidase and (**b**) β-galactosidase genes from various GH families in *E. rothschildi* between the two seasons

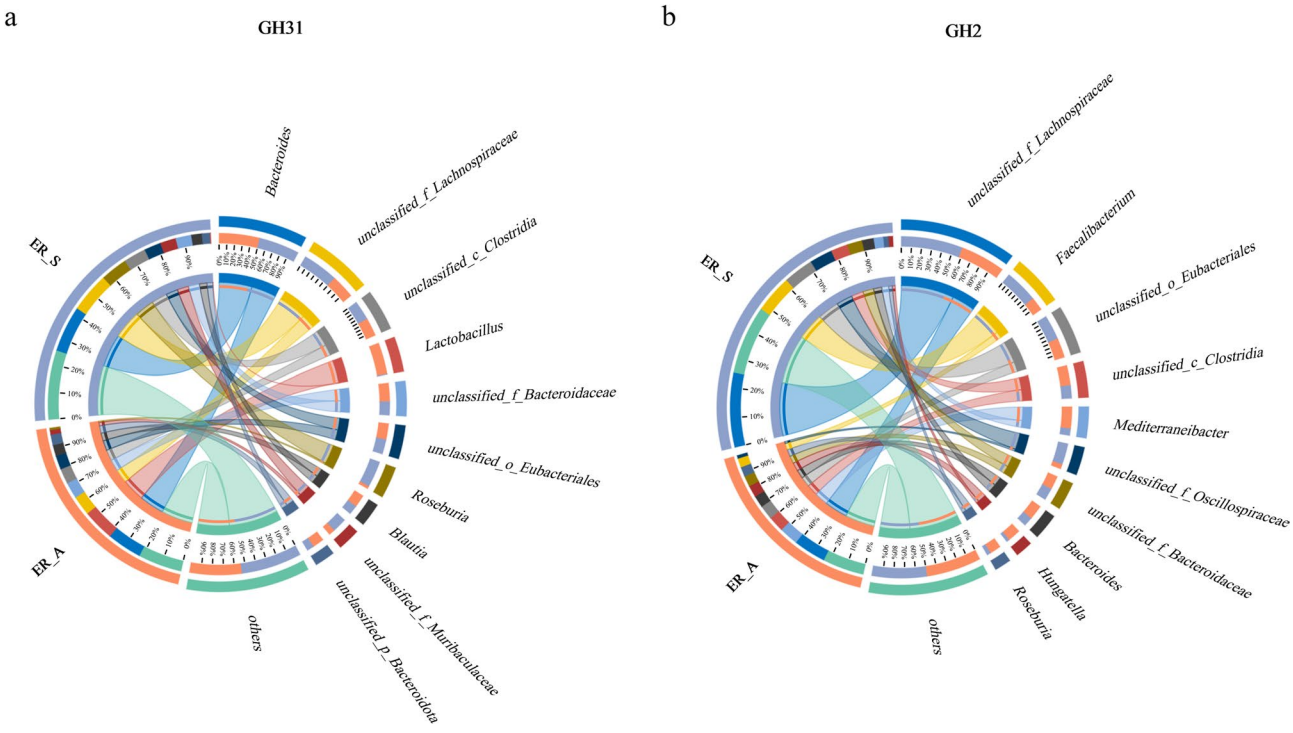

Fig. 4 Distribution of the dominant bacterial genera encoding differentially abundant genes for (**a**) α-galactosidase and (**b**) β-galactosidase from various GH families

the family level was presented in Fig. S9. As shown in Fig. S8 and Fig. S9, Muribaculaceae, Lachnospiraceae, and Oscillospiraceae were the main families in the intestinal microbes of *E. rothschildi*. Family-level taxonomic classification via Kraken2 revealed these three families as dominant families (Fig. S2). The bin-based taxonomic profiles partially recapitulate the overall community structure annotated by Kraken2, particularly for dominant microbial taxa. PCoA based on the relative abundance of all bins showed a clear separation between the two seasons (Fig. S10, PERMANOVA, $p < 0.05$).

Microbial community assembly analysis

Phylogenetic bin-based null model analysis was performed to calculate pairwise βNTI and RCI across samples, which collectively assess the relative contribution of deterministic versus stochastic processes in microbial community assembly. Summer samples exhibited significantly higher βNTI values (1.50 ± 0.92) than those in autumn samples (0.54 ± 0.75; Fig. S11, $p < 0.05$), with one sample showing $\beta NTI > 2$. This pattern indicated intensified heterogeneous selection during summer. This suggests the combined role of deterministic and stochastic processes in microbial assemblages in summer samples, and the dominant role of stochastic processes in autumn samples. Moreover, the results showed that the bacterial community pooled across the two seasons was shaped primarily by dispersal limitation, and drift (Fig. S12). Samples in autumn showed a higher relative contribution of drift compared to summer, implying that stochastic processes play a greater role in shaping the structure of the bacterial community in autumn. Additionally, the relative contribution of dispersal limitation was higher in autumn than summer, indicating a lower level of microbial exchange or dispersal across individuals within autumn. In addition, heterogeneous selection and homogeneous dispersal were just observed in summer samples. These results also indicated that both deterministic and stochastic processes played roles in microbial assemblages in summer samples.

Discussion

Comparison of composition and function of intestinal microbes of *E. rothschildi* between the two seasons

Seasonal shifts in the intestinal microbial composition of *E. rothschildi* indicated stronger carbohydrate-fermenting capacity in summer than autumn. As dominant phyla in the gut of *E. rothschildi* (Fig. 1a), Bacillota and Bacteroidota mediate carbohydrate fermentation [51]. In summer, *E. rothschildi* harbored a higher Bacillota/Bacteroidota ratio (Fig. 1c), enhancing energy extraction from dietary fibre in plants [52, 53]. At genus level, *Pseudoflavonifractor* was significantly more abundant in summer (Fig. 1 d). This butyrate-producing genus ferments complex carbohydrates to energize the colonic mucosa and exerts multiple regulatory functions in the host [54, 55].

Alpha diversity showed no seasonal differences (Fig. S3a, Wilcoxon rank sum test, $p > 0.05$), indicating that stable cellulose substrates in zokors' root diet sustain core microbiota (e.g., Firmicutes, Bacteroidetes) and alpha diversity stability. Nevertheless, seasonal dietary adjustments may alter functional microbiota ratios, causing significant seasonal differences in beta diversity (Fig. S3b, PERMANOVA, $R^2 = 0.2870$, $p < 0.05$).

KEGG pathway annotation revealed carbohydrate metabolism as a core function of intestinal microbes in *E. rothschildi* (Fig. 2a), aligning with the zokor's herbivorous diet dependent on plant-derived polysaccharides. Genes for carbohydrate metabolism increased in summer (Fig. S5), indicating enhanced carbohydrate-degradation capacity by the intestinal microbes in *E. rothschildi*. Within carbohydrate metabolism pathway, dominant galactose, starch and sucrose metabolism pathways were significantly enriched in *E. rothschildi* during summer (Fig. 2b). Within galactose metabolism pathway (ko00052), two most abundant enzymes, α-galactosidase (EC 3.2.1.22) and β-galactosidase (EC 3.2.1.23) were significantly enriched in summer (Fig. 2c). These results indicated enhanced carbohydrate degradation capacity in the intestinal microbes of *E. rothschildi* during summer versus autumn, particularly through galactose metabolism driven by α-galactosidase and β-galactosidase.

Habitat plant availability may drive functional adaptation in the intestinal microbes of *E. rothschildi* across seasons. Despite stable plant composition in its habitat, *E. rothschildi* may adjust foraging preferences to meet seasonal nutritional demands. Previous studies demonstrated that female plateau zokors forage aboveground for high-fat plants for nursing their pups in summer, suggesting elevated nutritional requirements during the breeding season [56, 57]. Therefore, enhanced capacity for galactose degradation in *E. rothschildi* during summer may represent an adaptation to special nutritional demands in breeding seasons.

Comparison of mean relative abundance of genes capable of encoding α-galactosidase or β-galactosidase

Carbohydrate-active enzymes (CAZymes) are crucial for degrading, modifying, and forming glycosidic bonds in carbohydrate metabolism [58]. As the predominant family among six protein families, glycoside hydrolases (GH) specialize in degrading complex polysaccharides. The present study focuses on genes from various GH families capable of encoding α-galactosidase and β-galactosidase. α-galactosidase, an exoglycosidase, hydrolyzes α-galactoside bonds to cleave terminal α-galactose residues from polysaccharides, glycolipids, and glycopeptides [59]. As the families capable of encoding α-galactosidase in *E. rothschildi* (Fig. 3a), previous studies confirmed that GH31 [60], GH4 [61, 62], GH57 [63, 64], GH36 [65, 66], GH97 [67, 68], GH27 [69, 70], and GH110 [71, 72] possessed α-galactosidase activities. Moreover, β-galactosidase is capable of hydrolyzing β-D-galactose residues and transferring galactosides [58]. Similarity, as the families capable of encoding β-galactosidases (Fig. 3b), GH1 [73], GH2 [74, 75], GH42 [76, 77], and GH35 [78–80] have been confirmed to possessed β-galactosidase activities.

Galactosidase genes from various GH families showed higher abundance in summer (Fig. 3), which is consistent with the increase abundance of galactose metabolism genes annotated in the KEGG database (Fig. 2c). These findings indicated an enhanced capacity of intestinal microbes in *E. rothschildi* to degrade galactose during summer.

Inference of dominant microbes encoding differentially abundant galactosidase genes from various GH families

In *E. rothschildi*, bacteria that were inferred to encode α-galactosidase genes from the GH31 family, including *Bacteroides*, *unclassified_f_Lachnospiraceae*, *unclassified_c_Clostridia*, *Roseburia*, were more abundant in summer than in autumn (Fig. 4a). Furthermore, bacteria inferred to encode β-galactosidase genes from the GH2 family, such as *unclassified_f_Lachnospiraceae*, *Faecalibacterium*, and *unclassified_o_Eubacteriales*, also exhibited higher summer abundances (Fig. 4b). Previous studies demonstrated that the genus *Bacteroides* harbored genes encoding both α-galactosidase and β-galactosidase [81, 82]. Furthermore, species belonging to *Roseburia* [83] and Lachnospiraceae [84] have been reported to produce α-galactosidase, whereas *Faecalibacterium* was known to produce β-galactosidase [85]. In summer, increased abundances of specific microbes, including *Bacteroides*, *unclassified_f_Lachnospiraceae*, *Roseburia*, and *Faecalibacterium*, may promote galactose degradation in the intestinal microbes of *E. rothschildi*, given their galactose-degrading potential.

Microbial community assembly

Phylogenetic reconstruction was performed using 53 archaeal and 120 bacterial conserved marker genes from GTDB release 214.1. Metagenome-assembled genomes (MAGs) were aligned against the corresponding conserved gene sets of bacteria or archaea to construct a phylogenomic tree. GTDB-Tk enables classification of the increasing number of microbial genomes from metagenomic studies [48, 86]. Independent validations confirm its accuracy in MAG taxonomic classification [87]. Within this phylogenetic framework, we employed null model analysis to quantify the relative contributions of deterministic versus stochastic processes in microbial community assembly.

Previous studies have suggested that during the assembly of microbial communities, deterministic and stochastic processes interact synergistically rather than being mutually exclusive [88, 89]. Null model analysis revealed seasonal variation in the intestinal microbial assembly of *E. rothschildi*. It was found that stochastic processes (e.g., ecological drift, dispersal limitation) govern the intestinal microbial assembly of *E. rothschildi* across seasons (Fig. S12). Seasonal variations significantly altered the contributions of heterogeneous selection, homogeneous dispersal, and dispersal limitation. Summer samples experienced stronger heterogeneous selection, thereby heightening combined effect of deterministic and stochastic processes, as elevated nutritional demands may have intensified host selection in the breeding season. While dispersal limitation shaped microbial communities in both seasons, its effect was stronger in autumn. Conversely, stochastic dominance in autumn may align with relaxed host selection.

In this study, we investigated the intestinal microbes of *E. rothschildi* across two different seasons. While these data provide initial clues regarding temporal variations, the interpretation of seasonal effects is subject to certain limitations. Sampling restricted to two time points limits our ability to determine whether the observed differences represent consistent seasonal dynamics versus year-specific anomalies. Furthermore, the small sample size may amplify the impact of individual heterogeneity on gut microbiome profiles. Thus, the causal linkage between observed microbial shifts and seasonal adaptation remains speculative.

To substantiate these preliminary observations, future studies should prioritize longitudinal monitoring over complete annual cycles, ideally extending across consecutive years. Increasing sample sizes ($n > 10$ per season) would enhance statistical power to distinguish seasonality from individual-level variation. Concurrent measurement of environmental covariates (e.g., food availability) and host physiological states (e.g., hormone levels) could further clarify the mechanisms underlying microbiome fluctuations.

Conclusion

In summary, this metagenomic study systematically investigated the seasonal dynamics of intestinal microbial composition, functional profiles, and assembly processes in *Eospalax rothschildi*. Our findings demonstrated that seasonality exerts a profound influence on both the intestinal microbial composition and function of *E. rothschildi*. Distinct shifts in microbial diversity and community structure were observed between seasons, with summer samples exhibiting a significant enrichment of microbes specializing in carbohydrate metabolism. Functional analyses further demonstrated enhanced carbohydrate degradation capacities during summer, particularly through the increase in the relative abundance of galactose metabolism pathways. This metabolic enhancement was mechanistically linked to elevated activities of α-galactosidase and β-galactosidase genes within these microbial populations, particularly *Bacteroides*, *unclassified_f_Lachnospiraceae*, *Roseburia*, and *Faecalibacterium*. Notably, the ecological assembly of intestinal microbes exhibited contrasting seasonal drivers: deterministic processes and stochastic forces jointly governed microbial community assembly in summer, whereas stochasticity emerged as the dominant factor in autumn. These results collectively establish season as a pivotal regulator of intestinal microbial ecology in *E. rothschildi*, shaping its taxonomic structure, metabolic functions, and assembly mechanisms.

Supplementary Information

The online version contains supplementary material available at https://doi.org/10.1186/s12866-025-04414-5.

Additional file 1: Fig. S1. Relative abundances of intestinal microbes of ***E. rothschildi*** between the two seasons at domain level based on the NR database. Fig. S2. Relative abundances of intestinal microbes of ***E. rothschildi*** between the two seasons at family level based on the NR database. Fig. S3. (a) The comparisons of alpha diversity of intestinal microbes of***E. rothschildi*** between the two seasons. (b) Principal coordinates analysis (PCoA) of bacterial communities of ***E. rothschildi*** across seven samples based on Bray-Curtis distance metrics. Fig. S4. Mean relative abundances of function of intestinal microbes of ***E. rothschildi*** between the two seasons based on the KEGG database. Fig. S5. Differences of intestinal microbial function of ***E. rothschildi*** between the two seasons at the second level under KEGG metabolism pathway. Fig. S6. Metabolic pathway associated with galactose metabolism in zokor (ko00052). Fig. S7. Mean relative abundances of function of intestinal microbes of ***E. rothschildi*** across all zokor samples based on the CAZy database. Fig. S8. Phylogenetic relationships and family-level taxonomy of 97 bins from the intestine of ***E. rothschildi*** across two seasons. Fig. S9. Relative abundances of bin-based intestinal microbes of ***E. rothschildi*** across seven samples at family level. Fig. S10. Bin-based principal coordinates analysis (PCoA) of bacterial communities of ***E. rothschildi*** across seven samples based on Bray-Curtis distance metrics. Fig. S11. Comparisons of betaMNTD values of intestinal microbes of ***E. rothschildi*** between the two seasons. Fig. S12. Summary of the relative contributions of the ecological processes that determine community assembly between the two seasons.

Additional file 2: Table S1. Sample information. Table S2. Summary statistics on sequence quality control and assembly of each sample. Table S3. Quality assessment and taxonomic classification of the MAGs.

Acknowledgements

We sincerely thank Forest Pest Control Station of Hanzhong city for collecting samples of ***Eospalax rothschildi.***

Authors' contributions

Y Zou, CX Han and YS Wang wrote the main manuscript text. CX Han collected samples and data. YS Wang analyzed the data. Y Zou and Q Zou prepared figure 1~4. All authors reviewed the manuscript.

Funding

This work was supported by Youth Found of the National Natural Science Foundation of China (62402344), and the National Natural Science Foundation of China (62531002, 62373080). The funding bodies provided all the help in the data analysis and interpretation of data.

Data availability
All raw reads have been submitted and archived in the NCBI Short Read Archive (SRA) under the BioProject identifiers PRJNA857464 (summer) and PRJNA1134278 (autumn).

Declarations

Ethics approval and consent to participate
All the animal experiments were approved by the Ethics Committee of University of Electronic Science and Technology of China (Approval Code: 106142024103031567). The processing of wild animals and sample collection were strictly congruent with the guidelines of our academic institution.

Consent for publication
Not applicable.

Competing interests
The authors declare no competing interests.

Received: 25 March 2025 / Accepted: 22 September 2025
Published online: 28 October 2025

References

1. Qin J, Li R, Raes J, Arumugam M, Burgdorf KS, Manichanh C, Nielsen T, Pons N, Levenez F, Yamada T. A human gut microbial gene catalogue established by metagenomic sequencing. Nature. 2010;464:59.
2. Brahe LK, Astrup A, Larsen LH. Can we prevent obesity-related metabolic diseases by dietary modulation of the gut microbiota? Adv Nutr. 2016;7:90–101.
3. Bevins CL, Salzman NH. Paneth cells, antimicrobial peptides and maintenance of intestinal homeostasis. Nat Rev Microbiol. 2011;9:356–68.
4. Thomas F, Hehemann JH, Rebuffet E, Czjzek M, Michel G. Environmental and gut bacteroidetes: the food connection. Front Microbiol. 2011;2:93.
5. Wang Y, Wang M, Chen J, Li Y, Kuang Z, Dende C, et al. The gut microbiota reprograms intestinal lipid metabolism through long noncoding RNA Snhg9. Science. 2023;381:851–7.
6. Hu S, Bourgonje AR, Gacesa R, Jansen BH, Björk JR, Bangma A, et al. Mucosal host-microbe interactions associate with clinical phenotypes in inflammatory bowel disease. Nat Commun. 2024;15:1470.
7. Eshleman EM, Rice T, Potter C, Waddell A, Hashimoto-Hill S, Woo V, et al. Microbiota-derived butyrate restricts tuft cell differentiation via histone deacetylase 3 to modulate intestinal type 2 immunity. Immunity. 2024;57:319–32.
8. Clemente JC, Ursell LK, Parfrey LW, Knight R. The impact of the gut microbiota on human health: an integrative view. Cell. 2012;148:1258–70.
9. Murugesan S, Nirmalkar K, Hoyo-Vadillo C, Garcia-Espitia M, Ramirez-Sanchez D, Garcia-Mena J. Gut Microbiome production of short-chain fatty acids and obesity in children. Eur J Clin Microbiol Infect Dis. 2017;37:621–5.
10. Tremaroli V, Bäckhed F. Functional interactions between the gut microbiota and host metabolism. Nature. 2012;489:242–9.
11. Flint H, Scott K, Louis P, Dunan S, et al. The role of the gut microbiota in nutrition and health. Nat Reviews Gastroenterol Hepatol. 2012;9:577–89.
12. Hird SM. Evolutionary biology needs wild microbiomes. Front Microbiol. 2017;8:725.
13. Bonder MJ, Kurilshikov A, Tigchelaar EF, Mujagic Z, Imhann F, Vila AV, et al. The effect of host genetics on the gut Microbiome. Nat Genet. 2016;48:1407–12.
14. Maynard CL, Elson CO, Hatton RD, Weaver CT. Reciprocal interactions of the intestinal microbiota and immune system. Nature. 2012;489:231–41.
15. Langille MGI, Meehan CJ, Koenig JE, Dhanani AS, Rose RA, Howlett SE, et al. Microbial shifts in the aging mouse gut. Microbiome. 2014;2:1–12.
16. Sender R, Fuchs S, Milo R. Revised estimates for the number of human and bacteria cells in the body. PLoS Biol. 2016;14:e1002533.
17. Nicholson JK, Holmes E, Kinross J, Burcelin R, Gibson G, Jia W, et al. Host-gut microbiota metabolic interactions. Science. 2012;336:1262–7.
18. Dominianni C, Sinha R, Goedert JJ, Pei Z, Yang L, Hayes RB, et al. Sex, body mass index, and dietary fiber intake influence the human gut Microbiome. PLoS ONE. 2015;10:e0124599.
19. Carmody RN, Gerber GK, Luevano JM, Gatti DM, Somes L, Svenson KL, et al. Diet dominates host genotype in shaping the murine gut microbiota. Cell Host Microbe. 2015;17:72–84.
20. Ren T, Boutin S, Humphrie MM, Dantzer B, Gorrell JC, Coltman DW, Mcadam AG, Wu M. Seasonal, spatial, and maternal effects on gut Microbiome in wild red squirrels. Microbiome. 2017;5:163.
21. Zou Y, Han C, Zhang X, Nan X. The associations between intestinal bacteria of Eospalax Cansus and soil bacteria of its habitat. BMC Vet Res. 2022;18:1–11.
22. Shah T, Hou Y, Jiang J, Shah Z, Wang Y, Li Q, et al. Comparative analysis of the intestinal Microbiome in rattus norvegicus from different geographies. Front Microbiol. 2023;14:1283453.
23. Ley RE, Hamady M, Lozupone C, Turnbaugh PJ, Ramey RR, Bircher JS, et al. Evolution of mammals and their gut microbes. Science. 2008;320:1647–51.
24. Li G, Li J, Kohl KD, Yin B, Wei W, Wan X, et al. Dietary shifts influenced by livestock grazing shape the gut microbiota composition and co-occurrence networks in a local rodent species. J Anim Ecol. 2019;88:302–14.
25. Huang X, Mi J, Denman SE, Basangwangdui, Pingcuozhandui, Zhang Q, et al. Changes in rumen microbial community composition in Yak in response to seasonal variations. J Appl Microbiol. 2022;132:1652–65.
26. Xia T, Yao Y, Wang C, Dong M, Wu Y, Li D, et al. Seasonal dynamics of gut microbiota in a cohort of wild Tibetan macaques (Macaca thibetana) in Western China. Global Ecol Conserv. 2021;25:e01409.
27. Fan C, Zhang L, Jia S, Tang X, Fu H, Li W, et al. Seasonal variations in the composition and functional profiles of gut microbiota reflect dietary changes in plateau Pikas. Integr Zool. 2022;17:379–95.
28. Li BG, Chen FG. The phylogeny, speciation and original center of Eospalax. J Norwest Univ (nature science edition). 1986;16:59–66.
29. Wei WH, Zhou WY. Comparison of the behaviors of plateau Zokor during the breeding and non-breeding periods. Acta Theriol Sinica. 1996;16:194–201.
30. An K, Yao B, Tan Y, Kang Y, Wang Z, Su J. Spermatocytes are the terminals of germ cell differentiation in plateau Zokor (*Eospalax baileyi*) during the non-breeding season. Integr Zool. 2025;20:608–22.
31. Liu K. Impact on vegetation and soil from seasonal activities of the prairie mole rat (Myospalax aspalax Pallas). [Master's thesis]. Inner Mongolia Agricultural University. 2014.
32. Bolger AM, Lohse M, Usadel B, Trimmomatic. A flexible trimmer for illumina sequence data. Bioinformatics. 2014;30:2114–20.
33. Langmead B, Salzberg SL. Fast gapped-read alignment with bowtie 2. Nat Methods. 2012;9:357–9.
34. Li D, Liu CM, Luo R, Sadakane K, Lam TW. MEGAHIT: an ultra-fast single-node solution for large and complex metagenomics assembly via succinct de Bruijn graph. Bioinformatics. 2015;31:1674–6.
35. Hyatt D, Chen GL, LoCascio PF, Land ML, Larimer FW, Hauser LJ, et al. Prodigal: prokaryotic gene recognition and translation initiation site identification. BMC Bioinformatics. 2010;11:1–11.
36. Fu L, Niu B, Zhu Z, Wu S, Li W. CD-HIT: accelerated for clustering the next-generation sequencing data. Bioinformatics. 2012;28:3150–2.
37. Li W, Godzik A. Cd-hit: a fast program for clustering and comparing large sets of protein or nucleotide sequences. Bioinformatics. 2006;22:1658–9.
38. Patro R, Duggal G, Love MI, Irizarry R, Kingsford C. Salmon provides fast and bias-aware quantification of transcript expression. Nat Methods. 2017;14:417–9.
39. Buchfink B, Xie C, Huson DH. Fast and sensitive protein alignment using DIAMOND. Nat Methods. 2015;12:59–60.
40. Wood D, Salzberg S. Kraken: ultrafast metagenomic sequence classification using exact alignments. Genome Biol. 2014;15:R46.
41. Lu J, Breitwieser FP, Thielen P, Salzberg SL. Bracken: estimating species abundance in metagenomics data. PeerJ Comput Sci. 2017;3:e104.
42. Kanehisa M, Goto S. KEGG: Kyoto encyclopedia of genes and genomes. Nucleic Acids Res. 2000;28:27–30.
43. Huerta-Cepas J, Forslund K, Coelho LP, Szklarczyk D, Jensen LJ, Von Mering C, Bork P. Fast genome-wide functional annotation through orthology assignment by eggNOG-mapper. Mol Biol Evol. 2017;34:2115–22.
44. Kang DD, Li F, Kirton E, Thomas A, Egan R, An H, Wang Z. MetaBAT2: an adaptive Binning algorithm for robust and efficient genome reconstruction from metagenome assemblies. Peer J. 2019;7:e7359.
45. Parks DH, Rinke C, Chuvochina M, Chaumeil PA, Woodcroft BJ, Evans PN, et al. Recovery of nearly 8,000 metagenome-assembled genomes substantially expands the tree of life. Nat Microbiol. 2017;2:1533–42.
46. Parks DH, Imelfort M, Skennerton CT, Hugenholtz P, Tyson GW. CheckM: assessing the quality of microbial genomes recovered from isolates, single cells, and metagenomes. Genome Res. 2015;25:1043–55.
47. Olm MR, Brown CT, Brooks B, Banfield JF. dRep: a tool for fast and accurate genomic comparisons that enables improved genome recovery from metagenomes through de-replication. ISME J. 2017;11:2864–8.

48. Chaumeil PA, Mussig AJ, Hugenholtz P, Parks DH. GTDB-Tk: A toolkit to classify genomes with the genome taxonomy database. Bioinformatics. 2020;36:1925–7.
49. Ning D, Yuan M, Wu L, Zhang Y, Guo X, Zhou X, et al. A quantitative framework reveals ecological drivers of grassland microbial community assembly in response to warming. Nat Commun. 2020;11:4717.
50. Stegen JC, Lin X, Fredrickson JK, Chen X, Kennedy DW, Murray CJ, et al. Quantifying community assembly processes and identifying features that impose them. ISME J. 2013;7:2069–79.
51. Ley RE, Peterson DA, Gordon JI. Ecological and evolutionary forces shaping microbial diversity in the human intestine. Cell. 2006;124:837–48.
52. Steelman SM, Chowdhary BP, Dowd S, Suchodolski J, Janečka JE. Pyrosequencing of 16S rRNA genes in fecal samples reveals high diversity of hindgut microflora in horses and potential links to chronic laminitis. BMC Vet Res. 2012;8:1–11.
53. Liu XF, Fan HL, Ding XB, Hong ZS, Nei YW, Liu ZW, Li GP, Guo H. Analysis of the gut microbiota by high-throughput sequencing of the V5-V6 regions of the 16S rRNA gene in Donkey. Curr Microbiol. 2014;68:657–62.
54. Luo YH, Peng HW, Wright AD, Bai SP, Ding XM, Zeng QF, et al. Broilers fed dietary vitamins harbor higher diversity of cecal bacteria and higher ratio of Clostridium, Faecalibacterium, and Lactobacillus than broilers with no dietary vitamins revealed by 16S rRNA gene clone libraries. Poult Sci. 2013;92:2358–66.
55. Liu Q, Zhang Z, Ji P, Liu J, Chen B, Mingyao E, et al. Ginseng polysaccharide components attenuate obesity and liver lipid accumulation by regulating fecal microbiota and hepatic lysine degradation. Int J Biol Macromol. 2024;269:131872.
56. Chu B, Ji C, Zhou J, Zhou Y, Hua L. Why does the plateau Zokor (Myospalax fontanieri: rodentia: Spalacidae) move on the ground in summer in the Eastern Qilian mountains? J Mammal. 2021;102:346–57.
57. Zhang Y. The biology and ecology of plateau Zokors (Eospalax fontanierii). In: Begall S, Burda H, Schleich CE, editors. Subterranean rodents: news from underground. Berlin/Heidelberg, Germany: Springer; 2007. pp. 237–49.
58. Lombard V, Ramulu HG, Drula E, Coutinho PM, Henrissat B. The carbohydrate-active enzymes database (CAZy) in 2013. Nucleic Acids Res. 2014;42:D490–5.
59. Desnick RJ, Ioannou YA, Eng CM, α-Galactosidase A. deficiency: Fabry disease, in: Scriver CR, Beaudet AL, Sly WS, Valle D, Kinzler KE, Vogelstein B, editors. The Metabolic and Molecular Bases of Inherited Disease, 8th ed. McGraw-Hill, New York; 2001. p. 3733–3774.
60. Miyazaki T, Ishizaki Y, Ichikawa M, Nishikawa A, Tonozuka T. Structural and biochemical characterization of novel bacterial α-galactosidases belonging to glycoside hydrolase family 31. Biochem J. 2015;469:145–58.
61. Chakladar S, Cheng L, Choi M, Liu J, Bennet AJ. Mechanistic evaluation of mela α-galactosidase from citrobacter freundii: a family 4 Glycosyl hydrolase in which oxidation is rate-limiting. Biochemistry. 2011;50:4298–308.
62. Morabbi Heravi K, Watzlawick H, Altenbuchner J. The MelREDCA Operon encodes a utilization system for the raffinose family of oligosaccharides in Bacillus subtilis. J Bacteriol. 2019;201:10–1128.
63. Duffaud GD, McCutchen CM, Leduc P, Parker KN, Kelly RM. Purification and characterization of extremely thermostable β-mannanase, β-mannosidase, and α-galactosidase from the hyperthermophilic Eubacterium thermotoga Neapolitana 5068. Appl Environ Microbiol. 1997;63:169–77.
64. Van Lieshout JF, Verhees CH, Ettema TJ, van der Sar S, Imamura H, Matsuzawa H, et al. Identification and molecular characterization of a novel type of α-galactosidase from Pyrococcus furiosus. Biocatal Biotransform. 2003;21:243–52.
65. Goulas T, Goulas A, Tzortzis G, Gibson GR. A novel α-galactosidase from Bifidobacterium bifidum with transgalactosylating properties: gene molecular cloning and heterologous expression. Appl Microbiol Biotechnol. 2009;82:471–7.
66. Peters S, Egert A, Stieger B, Keller F. Functional identification of Arabidopsis ATSIP2 (At3g57520) as an alkaline α-galactosidase with a substrate specificity for raffinose and an apparent sink-specific expression pattern. Plant Cell Physiol. 2010;51:1815–9.
67. Okuyama M, Kitamura M, Hondoh H, Kang MS, Mori H, Kimura A, et al. Catalytic mechanism of retaining α-galactosidase belonging to glycoside hydrolase family 97. J Mol Biol. 2009;392:1232–41.
68. Kikuchi A, Okuyama M, Kato K, Osaki S, Ma M, Kumagai Y, et al. A novel glycoside hydrolase family 97 enzyme: bifunctional β-L-arabinopyranosidase/α-galactosidase from bacteroides Thetaiotaomicron. Biochimie. 2017;142:41–50.
69. Tapernoux-Luthi EM, Böhm A, Keller F. Cloning, functional expression, and characterization of the raffinose oligosaccharide chain elongation enzyme, Galactan: Galactan galactosyltransferase, from common bugle leaves. Plant Physiol. 2004;134:1377–87.
70. Wang H, Ma R, Shi P, Huang H, Yang P, Wang Y, et al. Insights into the substrate specificity and synergy with mannanase of family 27 α-galactosidases from Neosartorya fischeri P1. Appl Microbiol Biotechnol. 2015;99:1261–72.
71. Liu QP, Yuan H, Bennett EP, Levery SB, Nudelman E, Spence J, et al. Identification of a GH110 subfamily of α1, 3-galactosidases: novel enzymes for removal of the α3Gal xenotransplantation antigen. J Biol Chem. 2008;283:8545–54.
72. McGuire BE, Hettle AG, Vickers C, King DT, Vocadlo DJ, Boraston AB. The structure of a family 110 glycoside hydrolase provides insight into the hydrolysis of α-1, 3-galactosidic linkages in λ-carrageenan and blood group antigens. J Biol Chem. 2020;295:18426–35.
73. Mangiagalli M, Lotti M. Cold-active β-galactosidases: insight into cold adaptation mechanisms and biotechnological exploitation. Mar Drugs. 2021;19:43.
74. Jacobson RH, Zhang XJ, DuBose RF, Matthews BW. Three-dimensional structure of β-galactosidase from E. coli. Nature. 1994;369:761–6.
75. Lu L, Li Z, Xiao M. Recent progress on galacto-oligosaccharides synthesis by microbial β-galactosidase–a review. Acta Microbiol Sinica. 2008;48:980–5.
76. Breton C, Šnajdrová L, Jeanneau C, Koča J, Imberty A. Structures and mechanisms of glycosyltransferases. Glycobiology. 2006;16:R29–37.
77. Hidaka M, Fushinobu S, Ohtsu N, Motoshima H, Matsuzawa H, Shoun H, Wakagi T. Trimeric crystal structure of the glycoside hydrolase family 42 β-galactosidase from thermus thermophilus A4 and the structure of its complex with galactose. J Mol Biol. 2002;322:79–91.
78. Zinin AI, Eneyskaya EV, Shabalin KA, Kulminskaya AA, Shishlyannikov SM, Neustroev KN. 1-O-Acetyl-β-D-galactopyranose: a novel substrate for the transglycosylation reaction catalyzed by the β-galactosidase from penicillium Sp. Carbohydr Res. 2002;337:635–42.
79. Gamauf C, Marchetti M, Kallio J, Puranen T, Vehmaanperä J, Allmaier G, et al. Characterization of the bgal-encoded glycosidehydrolase family 35 β-galactosidase of hypocrea jecorina with galacto-β-d-galactanase activity. FEBS J. 2007;274:1691–700.
80. Tanthanuch W, Chantarangsee M, Maneesan J, Ketudat-Cairns J. Genomic and expression analysis Ofglycosyl hydrolase family 35 genes from rice (Oryza sativa L). BMC Plant Biol. 2008;8:84.
81. Chaudet MM, Allen JL, Rose DR. Expression and purification of two family gh31 α-glucosidases from bacteroides Thetaiotaomicron. Protein Expression Purif. 2012;86:135–41.
82. Chia LW, Mank M, Blijenberg B, Aalvink S, Bongers R, Stahl B, et al. Bacteroides Thetaiotaomicron fosters the growth of butyrate-producing Anaerostipes caccae in the presence of lactose and total human milk carbohydrates. Microorganisms. 2020;8:1513.
83. La Rosa SL, Leth ML, Michalak L, Hansen ME, Pudlo NA, Glowacki R, et al. The human gut firmicute roseburia intestinalis is a primary degrader of dietary β-mannans. Nat Commun. 2019;10:905.
84. Rettenmaier R, Thieme N, Streubel J, Di Bello L, Kowollik ML, Huang L, et al. Variimorphobacter saccharofermentans gen. nov., sp. nov., a new member of the family Lachnospiraceae, isolated from a maize-fed biogas fermenter. Int J Syst Evol MicroBiol. 2021;71:005044.
85. Seo B, Jeon K, Baek I, Lee YM, Baek K, Ko G. Faecalibacillus intestinalis gen. nov., sp. nov. And Faecalibacillus faecis sp. nov., isolated from human faeces. Int J Syst Evol MicroBiol. 2019;69:2120–8.
86. Chaumeil PA, Mussig AJ, Hugenholtz P, Parks DH. GTDB-Tk v2: memory friendly classification with the genome taxonomy database. Bioinformatics. 2022;38:5315–6.
87. Coil DA, Jospin G, Darling AE, Wallis C, Davis IJ, Harris S, Eisen JA, Holcombe LJ, O'Flynn C. Genomes from bacteria associated with the canine oral cavity: A test case for automated genome-based taxonomic assignment. PLoS One. 2019; 14: e0214354.
88. Stegen JC, Lin X, Fredrickson JK, Konopka AE. Estimating and mapping ecological processes influencing microbial community assembly. Front Microbiol. 2015;6:370.
89. Nemergut DR, Schmidt SK, Fukami T, O'Neill SP, Bilinski TM, Stanish LF, et al. Patterns and processes of microbial community assembly. Microbiol Mol Biol Rev. 2013;77:342–56.

Publisher's Note